A New Simplified Two-Dimensional Model for the Threshold Voltage of MOSFET's with Nonuniformly Doped Substrate

Pole-Shang Lin, *Student Member, IEEE*, and Ching-Yuan Wu, *Member, IEEE*

Abstract—**A new simplified two-dimensional model for the threshold voltage of MOSFET's is derived in terms of simple characteristic functions. These characteristic functions are transformed from the exact series solution of the two-dimensional Poisson's equation, in which the effects of a nonuniformly doped substrate and a finite graded source–drain junction depth have been included. The attractive features of the developed model are: 1) charge-screening effects are proposed to account for the weak dependence of the threshold voltage on the substrate bias for short-channel MOSFET's, and 2) exact source and drain boundary potentials can be approximated by their equivalent power functions. The accuracy of the simplified 2-D model has been verified by 2-D numerical analysis. Moreover, comparisons between the simplified 2-D model and the experimental results have been made, and good agreement has been obtained for wide ranges of channel lengths, applied substrate, and drain biases.**

Nomenclature

- $\Psi(x, y)$ Two-dimensional potential distribution.
- $\epsilon_{si}(\epsilon_{ox})$ Dielectric permittivity of Si (SiO_2).
- N_{AB} Substrate doping concentration.
- $f(y)$ Nonuniform doping profile normalized by the substrate doping concentration.
- L Metallurgical channel length and length of the rectangular domain.
- y_d Minimum depletion depth and depth of the rectangular domain.
- T_{ox} Oxide thickness.
- C_{ox} Gate oxide capacitance per unit area.
- $\Psi(0, y)$ Source boundary potential.
- $\Psi(L, y)$ Drain boundary potential.
- k_m Eigenvalue of the Green function ($=(m\pi/L)$).
- $\rho_A(m)$ the Fourier coefficient of the charge density in the substrate [$=(1-(-1)^m)/m\pi(-2qN_{AB})$].
- $E(x, 0)$ Normal surface electric field [$= -(\partial/\partial y)\Psi(x, y)|_{y=o}$].
- $E(x, y_d)$ Normal electric field at the depletion edge [$= -(\partial/\partial y)\Psi(x, y)|_{y=y_d}$].
- V_T Threshold voltage.
- V_{GS} Gate–source voltage.
- V_{FB} Flat-band voltage.
- V_{DS} Drain–source voltage.
- V_{BS} Substrate–source voltage.
- x_m Location of the minimum surface potential
- ϕ_s Minimum surface potential.
- ϕ_{yd} Built-in voltage at the depletion edge with respect to the substrate.
- N_s^* Effective doping concentration viewed from the SiO_2–Si interface.
- N_d^* Effective doping concentration viewed from the depletion edge.
- $\overline{\Psi(x, 0)}$ Weighted surface potential.
- $\overline{E(x, 0)}$ Weighted normal surface electric field.
- $y_{JS}(y_{JD})$ Depletion edge of the source (drain) junction at the vertical boundary, as shown in Fig. 1.
- V_{BI} Built-in voltage between the source island and the substrate for zero substrate bias.
- N_{DIi} Implanted dose of the ith implantation.
- R_{pi} Projected range of the ith implantation.
- ΔR_{pi} Standard deviation (or straggle) of the implanted profile.
- N_{ASi} Concentration of the ith box profile.
- Y_{Si} Depth of the ith box profile.

Manuscript received March 14, 1989; revised November 8, 1990. This work was supported by the National Science Council, Taiwan, ROC, under Contract NSC 79-0416-E009-01. The review of this paper was arranged by Associate Editor K. C. Saraswat.

The authors are with the Institute of Electronics, College of Engineering, National Chiao-Tung University, Hsin-Chu, Taiwan, Republic of China.

IEEE Log Number 9042219.

I. Introduction

MOSFET device structures have become more and more sophisticated, and the development of a two-dimensional analytical model has become increasingly difficult due to the finite graded source–drain junction depth and the nonuniformly doped substrate. In the last decade, many analytical models for the threshold voltage of MOSFET's have been derived from the solution of the two-dimensional Poisson's equations [1]–[6]. However, the accuracy of a two-dimensional model strictly depends on both the degree of the approximation used for boundary conditions and the assumption made for obtaining the solution.

For a given set of boundary conditions, the solution techniques for the two-dimensional Poisson's equation in

0018-9383/91/0600-1376$01.00 © 1991 IEEE

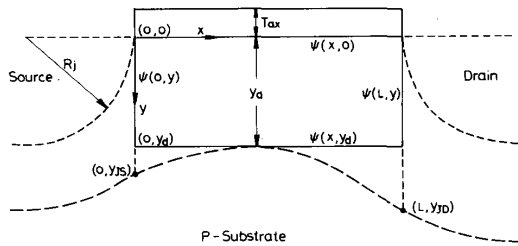

Fig. 1. The cross-sectional view of an n-channel MOSFET. The analytical solution is solved in the specified rectangular domain.

a MOSFET basically can be divided into two groups: one is through the technique of Laplace reduction [1]–[5] as first proposed by Ratnakumar and Meindl [1]; the other is through the Green function technique as proposed by Lin and Wu [6]. However, the threshold voltage models obtained by these techniques are expressed in a series form, and their practical applications are limited. Further simplifications of the final series expression for the threshold-voltage reduction have been made by Ratnakumar and Meindl [1] and Pfiester *et al.* [3]. However, their simplifications only keep the first term of the solution of a reduced Laplace equation and overlook the effects of the nonuniformly doped substrate and the graded source–drain junction.

In this work, a new simplified two-dimensional model for the threshold voltage of MOSFET's is presented. Based on the Green function technique [6], the exact series solution for the two-dimensional electric-field distribution is obtained in terms of a nonuniformly doped substrate, channel length, and source and drain boundary potentials. In Section II, we will present a new technique for reducing the complex series solution of the two-dimensional electric-field distribution into simple characteristic functions, which are the integrals of the effective doping concentration weighted by the hyperbolic-sine function. Then a new analytical threshold-voltage model can be obtained in terms of these simple characteristic functions. The attractive feature of our theoretical analysis is that the effects of the depletion charge density under the gate perturbed by the source and drain fields are replaced by an effective depletion charge density, in which the effects of nonuniformly doped substrate, effective channel length, and source and drain boundary potentials are included. Moreover, it will be shown that, due to the weighting effects of the hyperbolic-sine function, the effective depletion charge density is not completely controlled by the gate electrode, and the depth of the gate-controlled region is around the value of the channel length. This feature, which is known as the charge-screening effect, results in a weak substrate-bias dependence of the threshold voltage for a short-channel MOSFET. In Section III, the source and drain boundary potentials of a MOSFET with a finite graded source–drain junction depth are discussed. Since the effects of the source and drain boundary potentials on the threshold voltage are expressed in terms of their boundary integrals, two equivalent power functions for the source and drain boundary potentials are proposed, in which two coefficients can be determined by comparing the results obtained from 2-D numerical analysis if the source–drain boundary potential is given. In Section IV, the accuracy of the simplified 2-D model has been verified by the 2-D numerical analysis. Moreover, comparisons between the simplified 2-D model and the experimental results have been made, and good agreement has been obtained for wide ranges of channel lengths and applied drain–substrate biases. Finally, conclusions are given in Section V.

II. Model Formulation

A cross-sectional view of a MOSFET is shown in Fig. 1, where the x coordinate represents the direction along the SiO_2–Si interface and the y coordinate represents the direction perpendicular to the SiO_2–Si interface. The two-dimensional Poisson's equation to be solved in the *rectangular domain* is

$$\left(\frac{\partial^2}{\partial x^2} + \frac{\partial^2}{\partial y^2}\right)\Psi(x, y) = \frac{q}{\epsilon_{si}} N_{AB} f(y),$$

$$\text{for } 0 \leq y \leq y_d \text{ and } 0 \leq x \leq L \qquad (1)$$

and is subjected to the Dirichlet boundary conditions, $\Psi(x, 0)$, $\Psi(x, y_d)$, $\Psi(0, y)$, and $\Psi(L, y)$.

Using the Green's function technique [6], the potential distribution is expressed in terms of four boundary-potential integrals as

$$\Psi(x, y) = \Sigma \sin (k_m x) B_m(y) \qquad (2)$$

where

$$\begin{aligned} B_m(y) = & \frac{\rho_A(m)}{\epsilon_{si}} \int_0^{y_d} f(y')H(y; y'; k_m)\, dy' \\ & + \frac{2}{L} k_m \int_0^{y_d} \Psi(0, y')H(y; y'; k_m)\, dy' \\ & + \frac{2}{L} k_m \int_0^{y_d} \Psi(L, y')H(y; y'; k_m)\, dy' \\ & + \frac{\sinh k_m(y_d - y)}{\sinh (k_m y_d)} \frac{2}{L} \int_0^L \Psi(x', 0) \sin (k_m x')\, dx' \\ & + \frac{\sinh k_m y}{\sinh (k_m y_d)} \frac{2}{L} \int_0^L \Psi(x', y_d) \sin (k_m x')\, dx' \end{aligned} \qquad (3)$$

and

$$H(y; y'; k_m) = \begin{cases} \dfrac{\sinh (k_m y) \sinh [k_m(y_d - y')]}{k_m \sinh (k_m y_d)}, & \text{for } y < y' \\ \dfrac{\sinh (k_m y') \sinh [k_m(y_d - y)]}{k_m \sinh (k_m y_d)}, & \text{for } y' < y. \end{cases} \qquad (4)$$

with deriving this coefficient from the observation of particles' mean-square displacements or their velocity auto-

ory. This could not have been achieved with the alternative definition of temperature using the expectation value

Furthermore, the top and the bottom boundary potentials, $\Psi(x, 0)$ and $\Psi(x, y_d)$, are subjected to the following continuity equations:

$$E(x, 0) = [V_{GS} - V_{FB} - \Psi(x, 0)] C_{ox}/\epsilon_{si} \tag{5}$$

and

$$E(x, y_d) \cong 0 \tag{6}$$

where the normal electric field at the depletion edge is assumed to be zero. This approximation is reasonable because the equi-potential lines in the region beyond the minimum depletion edge y_d are nearly parallel to the y axis.

Using (2), the normal electric field at the SiO_2–Si interface and that at the depletion edge are given as

$$E(x, 0) = \Sigma \sin(k_m x) \frac{4}{L} S_m \tag{7}$$

and

$$E(x, y_d) = \Sigma \sin(k_m x) \frac{4}{L} D_m \tag{8}$$

where

$$\begin{aligned} S_m = {} & \frac{\cosh(k_m y_d)}{\sinh(k_m y_d)} \frac{k_m}{2} \int_0^L \Psi(x, 0) \sin(k_m x)\, dx \\ & - \frac{1}{\sinh(k_m y_d)} \frac{k_m}{2} \int_0^L \Psi(x, y_d) \sin(k_m x)\, dx \\ & - \frac{q}{\epsilon_{si}} \int_0^{y_d} \left\{ -N_{AB} f(y) + \frac{\epsilon_{si}}{q} k_m^2 [(\Psi(0, y) \right. \\ & \left. + \Psi(L, y)] \right\} \frac{\sinh[k_m(y_d - y)]}{k_m \sinh(k_m y_d)}\, dy \end{aligned}$$

$$\begin{aligned} D_m = {} & \frac{1}{\sinh(k_m y_d)} \frac{k_m}{2} \int_0^L \Psi(x, 0) \sin(k_m x)\, dx \\ & - \frac{\cosh(k_m y_d)}{\sinh(k_m y_d)} \frac{k_m}{2} \int_0^L \Psi(x, y_d) \sin(k_m x)\, dx \\ & + \frac{q}{\epsilon_{si}} \int_0^{y_d} \left\{ -N_{AB} f(y) + \frac{\epsilon_{si}}{q} k_m^2 [(\Psi(0, y) \right. \\ & \left. + \Psi(L, y)] \right\} \frac{\sinh(k_m y)}{k_m \sinh(k_m y_d)}\, dy. \end{aligned} \tag{10}$$

Since the normal electric fields in (7) and (8) are expanded in terms of the eigenfunction, $\sin(k_m x)$, the series forms can be simplified by the following orthogonal operation:

$$\overline{g(x)} = \frac{k_1}{2} \int_0^L g(x) \sin(k_1 x)\, dx \tag{11}$$

where the eigenfunction $\sin(k_1 x)$ is the weighting function and $g(x)$ is the function to be weighted.

Substituting (7) and (8) into (11), we obtain

$$\begin{aligned} \overline{E(x, 0)} = {} & \frac{q}{\epsilon_{si}} \int_0^{y_d} N_s^*(y) \frac{\sinh k_1(y_d - y)}{\sinh(k_1 y_d)}\, dy \\ & + \frac{\pi}{L} \frac{1}{\sinh(k_1 y_d)} [\overline{\Psi(x, 0)} - \overline{\Psi(x, y_d)}] \end{aligned} \tag{12}$$

and

$$\begin{aligned} \overline{E(x, y_d)} = {} & [\overline{\Psi(x, 0)} - \overline{\Psi(x, y_d)}] \\ & - \frac{q}{\epsilon_{si}} \int_0^{y_d} N_d^*(y) \frac{\sinh(k_1 y)}{k_1}\, dy \end{aligned} \tag{13}$$

where

$$\begin{aligned} N_s^*(y) = {} & N_{AB} f(y) - \frac{\epsilon_{si}}{2q} \left(\frac{\pi}{L}\right)^2 \\ & \cdot [\Psi(0, y) + \Psi(L, y) - 2\overline{\Psi(x, 0)}] \end{aligned} \tag{14}$$

and

$$\begin{aligned} N_d^*(y) = {} & N_{AB} f(y) - \frac{\epsilon_{si}}{2q} \left(\frac{\pi}{L}\right)^2 \\ & \cdot [\Psi(0, y) + \Psi(L, y) - 2\overline{\Psi(x, y_d)}]. \end{aligned} \tag{15}$$

The weighted top and bottom boundary potentials in the right side of (12)–(15), $\overline{\Psi(x, 0)}$ and $\overline{\Psi(x, y_d)}$, can be further simplified. It is known that the potential distribution along the x axis is a convex shape with the flat region near the central point ($x = L/2$), and the ratio of the convex parts to the channel region increases with decreasing the channel length. However, the weighting function is a concave shape with the zero values at the end points ($x = 0$, $x = L$). Therefore, the results of the weighted potentials are almost contributed by the parts around the central point ($x = L/2$) and are slightly increased with decreasing the channel length. The slight increase of $\overline{\Psi(x, 0)}$ and $\overline{\Psi(x, y_d)}$ with respect to the decrease of the channel length can be neglected as compared with those in the right side of (12)–(15). Therefore, the weighted potentials can be simply approximated by

$$\overline{\Psi(x, 0)} = \frac{\pi}{2L} \int_0^L \Psi(x, 0) \sin\left(\frac{\pi x}{L}\right) dx \cong \Psi(x_m, 0) = \phi_s \tag{16}$$

and

$$\begin{aligned} \overline{\Psi(x, y_d)} & = \frac{\pi}{2L} \int_0^L \Psi(x, y_d) \sin\left(\frac{\pi x}{L}\right) dx \\ & \cong \Psi(x_m, y_d) = \phi_{y_d} + V_{BS}. \end{aligned} \tag{17}$$

Based upon the above arguments, the weighted normal surface electric field in (12) can be written as

$$\begin{aligned} \overline{E(x, 0)} = {} & \frac{q}{\epsilon_{si}} \int_0^{y_d} N_s^*(y) \frac{\sinh k_1(y_d - y)}{\sinh(k_1 y_d)}\, dy \\ & + \frac{\pi}{L} \frac{1}{\sinh(k_1 y_d)} [\phi_s - (V_{BS} + \phi_{y_d})] \end{aligned} \tag{18}$$

and (14) can be expressed by

$$N_s^*(y) = N_{AB}f(y) - \frac{\epsilon_{si}}{2q}\left(\frac{\pi}{L}\right)^2 [\Psi(0, y) + \Psi(L, y) - 2\phi_s]. \tag{19}$$

The weighted normal surface electric field can also be obtained by substituting (5) into (11). Combining these two weighted normal surface fields, we obtain

$$[V_{GS} - V_{FB} - \overline{\Psi(x, 0)}]\, C_{ox}/\epsilon_{si} = \frac{q}{\epsilon_{si}} \int_0^{y_d} N_s^*(y) \frac{\sinh k_1(y_d - y)}{\sinh (k_1 y_d)} dy + \frac{\pi}{L} \frac{1}{\sinh (k_1 y_d)} [\phi_s - (V_{BS} + \phi_{y_d})]. \tag{20}$$

For short-channel MOSFET's, the above equation can be written as

$$[V_{GS} - V_{FB} - \overline{\Psi(x, 0)}]\, C_{ox}/\epsilon_{si} = \frac{q}{\epsilon_{si}} \int_0^{y_d} N_s^*(y) \exp\left(-\frac{\pi y}{L}\right) dy. \tag{21}$$

Note that the effective depletion charge density under the gate is obtained by weighting the effective doping concentration ($N_s^*(y)$) with an exponential decay function ($\exp(-(\pi/L)y)$). Therefore, there are two factors that exhibit the short-channel effects in our model: one is that some depletion charges under the gate are terminated by the electric fields emanating from the source–drain diffusion island, resulting in the decrease of the effective doping concentration ($N_s^*(y)$), as shown in (19); the other is that some electric fields emanating from the gate electrode may be terminated by the two vertical boundaries, and these parts increase with decreasing the channel length. As a result, the bulk depletion charges far away from the SiO_2/Si interface ($>L$) cannot be "seen" by the gate electrode, and this effect is described by the effective depletion charge density with $N_s^*(y)$ weighted by an exponential-decay function as shown in (21). Therefore, only the effective depletion charges near the surface region within the depth proportional to the channel length can terminate the electric field lines originated from the gate electrode. For this reason, if the depletion depth y_d is much larger than the channel length L, the normal surface electric field in a short-channel MOSFET is insensitive to the variations of the depletion depth y_d. This feature is called the *charge-screening effect*, which will result in a weak substrate-bias dependence for the threshold voltage of a short-channel MOSFET. This phenomenon is not well predicted by existing simplified two-dimensional models [1], [3], [7].

Similarly, combining (6), (13), (16), and (17), the bottom normal electric field in (13) can be written as

$$\phi_s - (\phi_{y_d} + V_{BS}) = \frac{q}{\epsilon_{si}} \int_0^{y_d} N_d^*(y') \frac{\sinh (k_1 y')}{k_1} dy' \tag{22}$$

and (15) can be expressed by

$$N_d^*(y') = N_{AB}f(y') - \frac{\epsilon_{si}}{2q}\left(\frac{\pi}{L}\right)^2 \cdot [\Psi(0, y') + \Psi(L, y') - 2V_{BS}] \tag{23}$$

where $N_d^*(y')$ is the effective doping concentration viewed from the bottom depletion edge and is expressed in terms of the substrate doping concentration, the effective channel length, and the source and drain boundary potentials. Based upon different mathematical treatments, Skotnicki *et al.* [7] proposed an effective doping formulation in terms of "current-line length" and doping profile in the curvilinear coordinate system. However, the effects of finite graded source–drain junction depth were not considered in their model. Note that (22) and (23) relate the potential difference between the channel surface and the bottom depletion edge to the effective depletion charge density under the gate. Because some electric field lines emanating from the source–drain island are terminated by the depletion charges under the gate, the effective depletion charge density (qN_d^*) under the gate is reduced. Therefore, the depletion depth y_d increases as the channel length decreases. Moreover, it should be noted that the approximations made in (16) and (17) will slightly underestimate the final solution of y_d when the channel length is very short. However, it has been stated previously that the normal surface electric field in a short-channel MOSFET is insensitive to the variations of y_d due to the charge-screening effect. Therefore, errors due to the above approximations can be neglected.

The threshold voltage is defined as the gate voltage at which the MOSFET is at the onset of strong inversion, i.e., $\phi_s = \phi_{s\,\text{inv}}$. Combining (20) and (22), the threshold voltage is given by

$$V_T = V_{FB} + \overline{\Psi(x, 0)}_{\text{inv}} + \frac{\epsilon_{si}}{C_{ox}} \overline{E(x, 0)}_{\text{inv}} \tag{24}$$

where the subscript "inv" denotes the onset of strong inversion. If $\Psi(0, y)$ and $\Psi(L, y)$ are known, the minimum depletion depth y_d can be determined from (22). Then, substituting y_d into (18), $\overline{E(x, 0)}_{\text{inv}}$ can be calculated. It will be shown in Section III that $\overline{\Psi(x, 0)}_{\text{inv}}$ in (24) can be simply replaced by $\phi_{s\,\text{inv}}$, and the lost term ($\overline{\Psi(x, 0)}_{\text{inv}} - \phi_{s\,\text{inv}}$) can be incorporated into the formulation of equivalent source–drain boundary potential.

Furthermore, it should be noted that the effective depletion charge density is weighted by a hyperbolic-sine function, and the transformed one-dimensional relation between the depletion charge density and the electric field/potential is quite different from that derived from the conventional 1-D coordinate system. However, for the long-channel case, (20) and (22) can be automatically reduced to those of the one-dimensional case derived by Brews [8]:

$$\phi_s - (\phi_{y_d} + V_{BS}) = \frac{q}{\epsilon_{si}} \int_0^{y_d} N_{AB}f(y')\, y'\, dy' \tag{25}$$

with deriving this coefficient from the observation of particles' mean-square displacements or their velocity auto-

ory. This could not have been achieved with the alternative definition of temperature using the expectation value

and

$$[V_{GS} - V_{FB} - \phi_s]C_{ox} = q \int_0^{y_d} N_{AB} f(y')\, dy'. \tag{26}$$

III. Simplified Source and Drain Boundary Potentials

The threshold-voltage model presented in the previous section has been derived in terms of the surface, the source, and the drain boundary potentials. For a MOS device with a nonuniformly doped substrate and finite depth of graded source–drain junction, the exact source and drain boundary potentials are difficult to analytically determine due to their two-dimensional nature [5]. It seems that this difficulty will limit the application of the derived threshold-voltage model. However, the derived threshold voltage expression depends only on the weighting values, namely, the weighted surface potential $\overline{\Psi(x, 0)}_{inv}$ and the weighted source–drain boundary potential. Since the weighting procedure is done through the integral operation and may smear the detailed form of the function, it is plausible to represent the exact source–drain boundary potential by an equivalent power function with the same integral value. Furthermore, the weighted surface potential $\overline{\Psi(x, 0)}_{inv}$, as discussed in the previous section, increases weakly with decreasing the channel length, and the potential $\overline{\Psi(x, 0)}_{inv}$ itself is a weighted function of the drain boundary potential [6]. Therefore, the term $\overline{\Psi(x, 0)}_{inv}$ in (24) can be simply replaced by $\phi_{s\,inv}$, and the lost term $(\overline{\Psi(x, 0)}_{inv} - \phi_{s\,inv})$ can be incorporated in the formulation of the drain boundary potential. As a result, the threshold voltage in (24) can be simplified as

$$V_T = V_{FB} + \phi_{s\,inv} + \frac{\epsilon_{si}\overline{E(x, 0)}_{inv}}{C_{ox}} \tag{27}$$

where the source and drain boundary potentials are represented by the equivalent power functions as

$$\Psi(0, y') = (V_{BI} - V_{BS})\left(1 - \frac{y'}{y_{JS}}\right)^n + \beta V_{BS}, \quad \text{for } y' \le y_{JS} \tag{28}$$

and

$$\Psi(L, y') = (V_{BI} - V_{BS} + \alpha V_{DS})\left(1 - \frac{y'}{y_{JD}}\right)^n + \beta V_{BS}, \quad \text{for } y' \le y_{JD}. \tag{29}$$

Note that the parameters α and β are introduced to adjust the weighted power functions to be equivalent to those calculated by the exact boundary potentials. Moreover, the parameter α is also used to correct the effect of the neglected term $(\overline{\Psi(x, 0)}_{inv} - \phi_{s\,inv})$ in the original threshold voltage model (24). Therefore, the parameter α is less than 1 even for the case of the source–drain island with an n^+ uniform doping profile. Furthermore, the order n is taken to be an integer so that the formulations in (18) and (22) can be analytically integrated. For simplicity, n is taken to be 2 and 3 for the substrate with uniform doping and nonuniform doping, respectively.

IV. Results and Discussions

In order to test the accuracy of the simplified threshold voltage model, comparisons with 2-D numerical analysis and experimental data have been made. The threshold voltage of the MOSFET's is deduced by the conventional extrapolation method at a drain voltage of 0.1 V, and the value of the drain current at the threshold voltage is denoted as the threshold current I_{DST}. For the large drain bias, the threshold voltage is determined as the gate voltage at which the normalized drain current is equal to the normalized threshold current $I^*_{DST}L/W$. The inversion criterion $\phi_{s\,inv}$ used in the threshold voltage model is determined by the extrapolation on the plot of inversion charge density versus V_{GS} [8], [9]. From the determined threshold voltage and inversion criterion $\phi_{s\,inv}$, the channel profile is approximated by a Gaussian profile, and its parameters can be determined and are listed in part (a) of Table I. For easy calculation of our threshold voltage model, the Gaussian profile can be further transformed into the equivalent box-profile [10] with the parameters listed in part (b) of Table I.

A. Comparisons with 2-D Numerical Analysis

The 2-D numerical analysis for MOSFET devices has been performed by an efficient MOS simulator–SUMMOS.[1] The channel profile used is a double Gaussian distribution, and its parameters for numerical simulation are listed in part (a) of Table I. For generality, the graded source–drain diffusion island with the junction depth R_j of 0.3 μm is taken. The numerical results for the drain boundary potential versus the vertical depth are shown in Fig. 2, in which the drain bias is 5.0 V and the substrate bias is varied from 0 to -4 V. The parameters α and β ($0 < \alpha$ and $\beta < 1$) in our simplified threshold voltage model are independent of device geometry, which can be determined simply by the trial-and-error approach or automatically searched by the nonlinear optimizer [11]. Comparisons between the 2-D numerical analysis and the developed threshold-voltage model are shown in Figs. 3 and 4. Fig. 3 shows the threshold voltage versus the substrate bias for different channel lengths, and Fig. 4 shows the threshold voltage versus the channel length for different substrate biases. It is clearly seen that good agreement has been obtained for wide ranges of substrate biases and channel lengths. Note that the parameter α ($=0.47$) used for simulation is smaller than 1. The reasons are mainly due to the effects of the graded source–drain junction and the correction of the omitted term $(\overline{\Psi(x, 0)}_{inv} - \phi_{s\,inv})$. Fig. 5 shows comparisons of the threshold-voltage reduc-

[1]The SUMMOS simulator is an efficient MOS device simulator developed by the Advanced Semiconductor Device and Technology Research Division, National Chiao-Tung University, Taiwan, Republic of China.

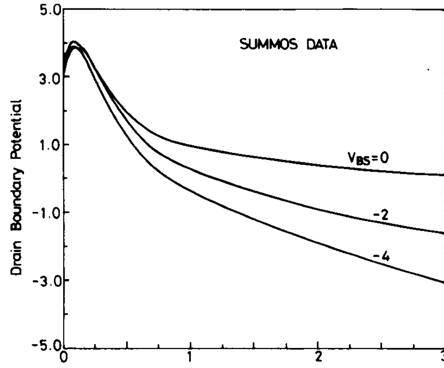

Fig. 2. The drain boundary potential $\Psi(L, y)$ versus the depth. The drain bias is 5.0 V and the substrate biases are 0, −2, and −4 V.

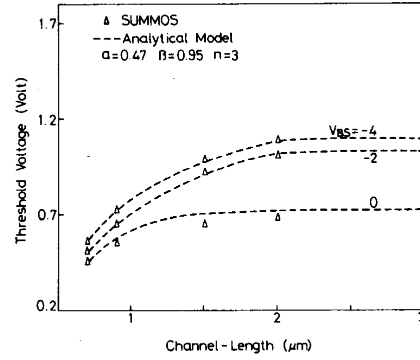

Fig. 4. The threshold voltage versus the channel length at the drain voltage of 5.0 V.

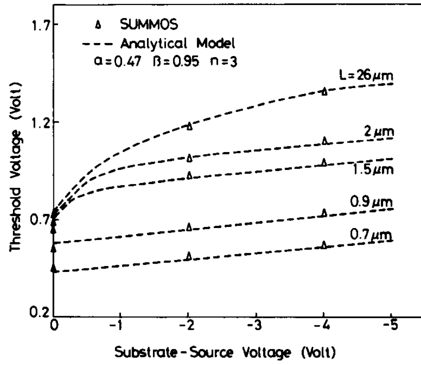

Fig. 3. The threshold voltage versus the substrate bias at a drain voltage of 5.0 V.

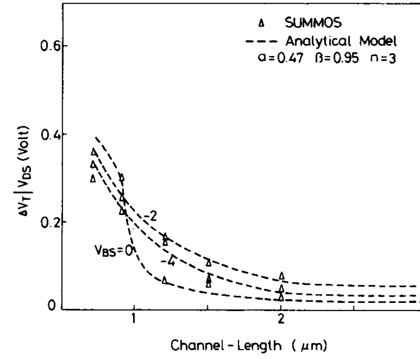

Fig. 5. The threshold-voltage reduction versus the channel length for different substrate biases.

TABLE I
(a) THE GAUSSIAN PARAMETERS USED FOR 2-D NUMERICAL SIMULATION. (b) THE EQUIVALENT BOX-PROFILE PARAMETERS USED FOR THE SIMPLIFIED THRESHOLD-VOLTAGE MODEL

	Device Parameter	Value
(a)	$N_{AB}(10^{14}\ \mathrm{cm}^{-3})$	3.00
	$N_{D l_1}(10^{11}\ \mathrm{cm}^{-2})$	7.75
	$\Delta R_{p_1}(10^{-5}\ \mathrm{cm})$	0.74
	$R_{P_1}(10^{-5}\ \mathrm{cm})$	1.27
	$N_{D I_2}(10^{11}\ \mathrm{cm}^{-2})$	3.43
	$\Delta R_{p_2}(10^{-5}\ \mathrm{cm})$	2.34
	$R_{P_2}(10^{-5}\ \mathrm{cm})$	5.56
(b)	$N_{AB}(10^{14}\ \mathrm{cm}^{-3})$	3.00
	$N_{AS1}(10^{16}\ \mathrm{cm}^{-3})$	2.753
	$Y_{S1}(10^{-4}\ \mathrm{cm})$	0.231
	$N_{AS2}(10^{16}\ \mathrm{cm}^{-3})$	0.448
	$Y_{S2}(10^{-4}\ \mathrm{cm})$	0.932

tion contributed by the drain voltage, and the threshold-voltage reduction is defined as

$$\Delta V_T|_{V_{DS}} = \frac{q}{\epsilon_{si}} \int_0^{y_d} \frac{\epsilon_{si}}{2q} \left(\frac{\pi}{L}\right)^2 [\Psi(L, y) - 2\phi_s] \frac{\sinh k_1(y_d - y)}{\sinh (k_1 y_d)} dy - (\overline{\Psi(x, 0)}_{\mathrm{inv}} - \phi_{s\mathrm{inv}}). \tag{30}$$

Note that the term $(\overline{\Psi(x, 0)}_{\mathrm{inv}} - \phi_{s\,\mathrm{inv}})$ is omitted in our simplified model, and its effect is incorporated in the equivalent drain boundary potential. The comparisons shown in Fig. 5, confirm our statement on the equivalent source–drain boundary potential in Section III. The charge-screening effect calculated from the developed threshold-voltage model is illustrated in Fig. 6, in which V_Q is the term contributed by the depletion charge density under the gate and is given by

$$V_Q = \frac{q}{\epsilon_{si}} \int_0^{y_d} N_{AB} f(y) \frac{\sinh k_1(y_d - y)}{\sinh (k_1 y_d)} dy + \frac{\pi}{L} \frac{1}{\sinh (k_1 y_d)} [\phi_s - (V_{BS} + \phi_{y_d})]. \tag{31}$$

Note that the function V_Q is almost independent of the substrate bias for short-channel MOSFET's, due to the charge-screening effect. The weak dependence of the threshold voltage on the substrate bias, as shown in Figs. 3 and 4, is due to the fact that the distribution of the

with deriving this coefficient from the observation of particles' mean-square displacements or their velocity auto-

ory. This could not have been achieved with the alternative definition of temperature using the expectation value

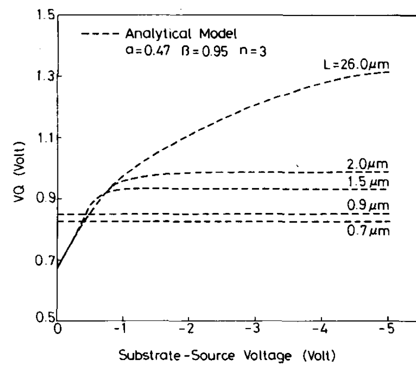

Fig. 6. The equivalent voltage V_Q contributed by the depletion charge density under the gate versus the substrate bias for different channel lengths.

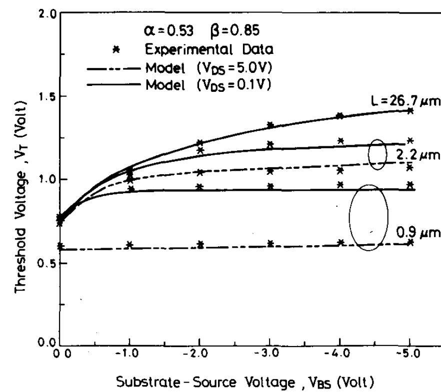

Fig. 7. The threshold voltage versus the substrate bias for different channel lengths and drain biases.

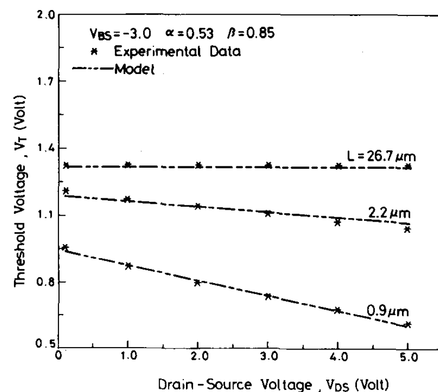

Fig. 8. The threshold voltage versus the drain voltage for different channel lengths and the substrate bias of −3 V.

source–drain boundary potential near the SiO_2–Si interface is a weak function of the substrate bias, as illustrated in Fig. 2.

B. Comparisons with the Experimental Results

In this section, the results of the simplified threshold-voltage model are compared with the experimental data measured from long- to short-channel n-MOSFET's with double-channel-boron implantations. The gate-oxide thickness (T_{ox}) and the source–drain junction depth of the fabricated MOS devices are 250 Å and 0.33 μm, respectively. The double-channel-boron implantations were performed through the gate oxide with an energy of 25 keV and a dose of $7.5 \times 10^{11}/cm^2$ for shallow implantation and an energy of 150 keV and a dose of $4.0 \times 10^{11}/cm^2$ for deep implantation. The source–drain junctions were implanted through thin oxide by using the energy of 60 keV and a dose of $6.0 \times 10^{15}/cm^2$. The parameters for the channel profile are listed in part (b) of Table I. Fig. 7 shows comparisons of the substrate-bias dependence of the threshold voltage between the simplified model and the experimental data for $V_{DS} = 0.1$ and 5 V. The dependence of the threshold voltage on the drain bias is also shown in Fig. 8, where the theoretical curves are obtained by linearizing the calculation points in Fig. 7. Note that the parameter α used for simulation is 0.53 (< 1), which is also used to compensate the effect of $(\Psi(x, 0)_{inv} - \phi_{s\ inv})$ on the threshold voltage reduction, as discussed in Section III. It is clearly seen that good agreement has been obtained for wide ranges of channel lengths, applied substrate and drain biases. In particular, the very weak-substrate-bias dependence of the threshold voltage for a short-channel MOSFET (for example, $L = 0.9\ \mu$m) is well predicted by our newly developed model.

V. Conclusion

A new simplified two-dimensional threshold-voltage model is presented in which the effects of channel length, nonuniformly doped substrate, and finite source–drain junction depth are included and characterized by simple characteristic functions. The source and drain boundary problems for modeling MOSFET's with a finite graded source–drain junction depth are treated by the equivalent power functions. One of the attractive features is that the maximum depth of the effective depletion region belonging to the gate electrode is approximately equal to the value of the channel length. This effect is known as the charge-screening effect and results in a weak dependence of the threshold voltage on the substrate bias for short-channel MOSFET's. The accuracy of the simplified threshold-voltage model for wide ranges of channel lengths and applied substrate–drain biases has been verified by comparison with the results of the 2-D numerical analysis and experimental MOSFET's having a nonuniformly doped substrate and a finite source–drain junction depth.

References

[1] K. N. Ratnakumar and J. D. Meindl, "Short-channel MOST threshold voltage model," *IEEE J. Solid-State Circuits*, vol. SC-17, no. 5, p. 937, 1982.

[2] D. R. Poole and D. L. Kwong, "Two-dimensional analytical modeling of threshold voltage of short-channel MOSFET's," *IEEE Electron Device Lett.*, vol. EDL-5, p. 443, 1984.

[3] J. R. Pfiester, J. D. Shott, and J. D. Meindl, "Performance limits of CMOS ULSI," *IEEE Trans. Electron Devices*, vol. ED-32, p. 333, 1985.
[4] J. D. Kendall and A. R. Boothroyd, "A two-dimensional analytical threshold voltage model for MOSFET's with arbitrarily doped substrates," *IEEE Electron Device Lett.*, vol. EDL-7, p. 401, 1986.
[5] V. Marash and R. W. Dutton, "Methodology for submicron device model development," *IEEE Trans. Computer-Aided Design of ICAS*, vol. 7, p. 299, 1988.
[6] P.-S. Lin and C.-Y. Wu, "A new approach to analytically solving the two-dimensional Poisson's equation and its application in short-channel MOSFET modeling," *IEEE Trans. Electron Devices*, vol. ED-34, no. 9, p. 1947, 1987.
[7] T. Skotnicki, G. Merckel, and T. Pedron, "The voltage-doping transformation: A new approach to the modeling of MOSFET short-channel effects," *IEEE Electron Device Lett.*, vol. 9, p. 109, 1988.
[8] J. R. Brews, "Threshold shifts due to nonuniform doping profile in surface channel MOSFET's," *IEEE Trans. Electron Devices*, vol. ED-26, p. 1696, 1979.
[9] D. A. Antoniadis, "Calculation of threshold voltage in nonuniformly doped MOSFET's," *IEEE Trans. Electron Devices*, vol. ED-31, no. 3, p. 303, 1984.
[10] S. Karmalker and K. N. Bhat, "The correct equivalent box representation for buried layer of BC MOSFET's in terms of the implantation parameters," *IEEE Electron Device Lett.*, vol. EDL-8, p. 457, 1987.
[11] M. S. Bazaraa and C. M. Shetty, *Nonlinear Programming—Theory and Algorithm*. New York: Wiley, 1979.

*

Pole-Shang Lin (S'85) was born in Taiwan, Republic of China, on May 29, 1960. He received the B.S. degree in electrical engineering from National Chiao-Tung University, Republic of China, in 1982 and the Ph.D. degree from the Institute of Electronics, National Chiao-Tung University, in 1989.

During 1982–1984, he was with the military and taught electronics at the Chinese Army Communication School. In 1989, he entered the Electronics Research and Service Organization of the Industrial Technology Research Institute. His research activities have been in the analytical modeling of short-channel MOS devices and poly-Si thin-film transistors. His present research interests focus on the small-geometry device simulation for VLSI.

Mr. Lin is a member of Phi Tau Phi.

*

Ching-Yuan Wu (S'69–M'72) was born in Taiwan, Republic of China, on March 18, 1946. He received the B.S. degree from the Department of Electrical Engineering, National Taiwan University, Taiwan, Republic of China, in 1968, and the M.S. and Ph.D. degrees from the State University of New York (SUNY) at Stony Brook, in 1970 and 1972, respectively.

During the 1968–1969 academic year, he served in the Chinese Air Force as a Second Lieutenant. During the 1972–1973 academic year, he was appointed as a Lecturer in the Department of Electrical Sciences, SUNY, Stony Brook. During the 1973–1975 academic years, he was a Visiting Associate Professor at National Chiao-Tung University (NCTU), Taiwan, Republic of China. In 1976, he became a Full Professor in the Department of Electronics and the Institute of Electronics, NCTU. During 1974–1980, he was the Director of the Engineering Laboratories and the Semiconductor Research Center, NCTU. He was a principal investigator of the National Electronics Mass Plan-Semiconductor Devices and Integrated-Circuit Technologies, during 1976–1979. He was the Director of the Institute of Electronics, NCTU, during 1978–1984. Since 1984, he has been the Dean, College of Engineering, NCTU. He has also been a Research Consultant of the Electronics Research and Service Organization (ERSO), ITRI, and an Academic Advisory Member of the Ministry of Education, Republic of China. His research activities have been in semiconductor device physics and modelings, and integrated-circuit design, and technologies. His present research interests focus on small-geometry devices in VLSI, CMOS latchup, new devices, and technologies. He has published over 140 papers in the semiconductor field.

Dr. Wu is a member of Phi Tau Phi and was recently appointed to the Honorary Editorial Advisory Board of *Solid-State Electronics*. He received the Academic Research Award in Engineering from the Ministry of Education (MOE), in 1979, and the outstanding Scholar award from the Chinese Educational and Cultural Foundation, Republic of China, in 1985. He received the outstanding research Professor fellowship from the MOE and the National Science Council (NSC), Republic of China, during 1982–1991.

with deriving this coefficient from the observation of particles' mean-square displacements or their velocity auto-

ory. This could not have been achieved with the alternative definition of temperature using the expectation value